A Local, Crossing-path Study of Attenuation and Anisotropy of the Inner Core

George Helffrich[1], Satoshi Kaneshima

Earth and Planetary Sciences, Tokyo Institute of Technology

J.-M. Kendall

Earth Sciences, University of Leeds, Leeds, UK

Short title: INNER CORE ATTENUATION AND ANISOTROPY

Abstract. We report results from studying a region under the north Pacific using 46 ray paths along east-west and north-south directions to study the nature of inner core anisotropy, and find an anisotropy signal in differential PKP_{BC}-PKP_{DF} at about the resolution of the data, with north-south paths faster than east-west, but no dependence of attenuation on wavespeed or depth in this part of the inner core. Inner core Q is 130^{+255}_{-52} between 140–340 km depth. The observations also provide constraints on the degree of homogeneous meridional anisotropy possibly present in the core, to between 0.1 and 0.6% velocity differences in the fast and slow directions, significantly smaller than the 2-4% axi-symmetric anisotropy in the inner core. The small meridional component to anisotropy argues against significant contributions to anisotropy from low-order inner core convection or stresses imposed on the inner core by the outer core field.

Introduction

Heterogeneity in inner core structure, superimposed in its large-scale anisotropy, is well-documented by various studies [*Su and Dziewonski*, 1995; *Kaneshima*, 1996; *Creager*, 1997; *Tanaka and Hamaguchi*, 1997; *Creager*, 1999; *Song*, 2000; *Niu and Wen*, 2001]. The inner core is also notable for its attenuation of high-frequency body waves, but evidence for radial and lateral variation in this property is more elusive, with some workers reporting radial variations [*Sacks*, 1971; *Doornbos*, 1974; *Tseng et al.*, 2001], and others not [*Niazi and Johnson*, 1992; *Bhattacharyya et al.*, 1993]. Radial or lateral heterogeneity in attenuation may be linked to anisotropy through a common physical process such as propagation through a textured, composite medium. The anisotropic attenuation results from scattering from oriented inclusions and the anisotropy due to the different polarizations interacting differently with the fabric that inclusions impose [*Doornbos*, 1974; *Peacock and Hudson*, 1990; *Cormier et al.*, 1998; *Kendall and Silver*, 1996]. *Souriau and Romanowicz* [1997] also cite the example of the anisotropic attenuation in sheet-silicate mineral composites, which, while not expected to exist in the inner core, provides an example of a material property that may also act in the solid core's iron alloy to link attenuation and anisotropy.

The joint variation in attenuation and anisotropy thus constrains the nature of the inner core. One attractive model among the many proposed to explain the inner core's anisotropy that also affects attenuation is liquid inclusions trapped in solid media [*Doornbos*, 1974; *Peacock and Hudson*, 1990]. Inefficient expulsion of outer core liquid as the inner core crystallizes is a viable way to produce this this texture [*Fearn et al.*, 1981; *Loper and Fearn*,

1983]. Despite its allure, it is not supported by the existing travel time and attenuation observations. *Souriau and Romanowicz* [1996, 1997] found that P wavespeed variation was fast where attenuation was largest, the opposite relation to the oriented inclusion model predictions. *Souriau and Romanowicz* [1997] proposed that intrinsic attenuation in the inner core's crystallites, oriented by convection, was operating in the inner core.

Low-order convection of the inner core or crystallite alignment due to the magnetic field in the inner or outer core [*Jeanloz and Wenk*, 1988; *Weber and Machetel*, 1992; *Karato*, 1993; *Romanowicz et al.*, 1996; *Bergman*, 1997; *Souriau and Romanowicz*, 1997; *Karato*, 1999] may contribute to the inner core's anisotropy. Either of these mechanisms orient the crystallites in the inner core along meridians of longitude. Averaged globally over all longitudes, a meridional form would be cylindrically symmetric, the form adopted at present for describing the core's anisotropy (see, e.g., *Creager* [1999]). Unlike the dependence of wavespeeds on ray angle with respect to the spin axis of the inner core in axisymmetric anisotropy, meridional anisotropy yields a wavespeed dependence on the local bottoming azimuth in the inner core. Thus the azimuthal dependence of wavespeed variations in the inner core at high angles to the spin axis provides a way to assess the relative strength of axisymmetric anisotropy to meridional anisotropy, and the mechanisms by which anisotropy arises in the inner core.

To investigate the anisotropy-attenuation relationship further and to assess any meridional contribution to anisotropy, we analyze broadband recordings of the core phases PKP$_{DF}$ and PKP$_{BC}$ in a restricted region of the inner core. Like *Souriau and Romanowicz* [1996], we use crossing ray paths and simultaneously analyze the attenuation and anisotropy of each record to establish the joint dependence of attenuation on inner core wavespeed. One set of directions

is north-south and the other is east-west through the study region in the inner core. We see a weak signature of anisotropy in the observations, at about the detection level, with north-south PKP$_{BC}$-PKP$_{DF}$ times slightly larger than east-west times, supporting anisotropy models derived from global data distributions. Evidence for a correlation between anisotropy and attenuation is weak in the datasset, and probably nonexistent. Within uncertainty, attenuation appears to be constant, independent of depth in this region of the inner core.

Data and Methods

The data are broadband recordings of PKP$_{DF}$ and PKP$_{BC}$ from the SPICeD array in the UK and Western Europe, the Freesia network in Japan, and the Global Seismic Network station TATO (Taiwan). SPICeD is a nine-station array operated for two years to study the core and the core-mantle boundary [*Kendall and Helffrich*, 2001]. Freesia is a permanent network of 30 stations operated by the National Research Institute of Earth Science and Disaster Prevention. Figure 1 shows a map of station locations and ray paths.

We measure PKP$_{BC}$-PKP$_{DF}$ differential times by hand-picking corresponding peaks and troughs in the respective waveforms [*Creager*, 1997]. While individual pick errors are ≤ 0.05 s (the data's sample rate), we estimate the differential time uncertainty to be the standard deviation of the mean of the pick differences in a single waveform, which is on average 0.25 s. We correct the residuals for ellipticity and reduce them to residuals δt with respect to AK135 [*Kennett et al.*, 1995].

The attenuation measurement method follows *Niazi and Johnson* [1992], via the spectral decay of PKP$_{DF}$ relative to PKP$_{BC}$. We window the two phases and assess whether scattering

from the CMB region contaminates the waveforms [*Bowers et al.*, 2000]. Within the windows

chosen, we calculate multitaper spectral estimates [*Park et al.*, 1987] using five 4π prolate

tapers. The time window immediately preceding the PKP$_{DF}$ arrival provides a noise estimate.

The spectra are smoothed and divided point-wise, retaining only points where both signals lie

above the noise level. The resulting set of points is fit to the model

$$ln\left[\frac{A_{DF}(f)}{A_{BC}(f)}\right] \;\; = \;\; a \;\; - \;\; bf \quad , \tag{1}$$

where f is frequency. The constant a represents differences in source amplitude for PKP$_{BC}$

and PKP$_{DF}$ and is not of interest, but the value of b is related to the inner core's t^* via

$t^* \;\; = \;\; b/\pi$. To estimate b, we use a robust line fitting method that minimizes the average

absolute deviation of the points from the best-fit line [*Press et al.*, 1992], and use jackknifing

to estimate the uncertainty in b, and thus t^* [*Efron and Tibishrani*, 1991]. $Q^{-1} \;\; = \;\; t^*/T$,

where T is the travel time across the inner core. Following *Widmer et al.* [1991], we report

$q \;\; \equiv \;\; 10000/Q$ rather than Q because the uncertainty in b propagates linearly into this value,

and for typographical ease.

Results

To simplify the discussion of the results, we will call the Tonga-Fiji to SPICeD array

observations the "SPICeD data," and the rest the "Asian data." The SPICeD data paths thread

the inner core along northerly azimuths, whereas the Asian data paths travel east-west (Figure

1). Both bottom in the same region of the inner core, and thus sample similar parts of the core

but along orthogonal azimuths. This provides an ideal geometry to assess the existence of

either axi-symmetric or meridional inner core anisotropy.

Figure 2 shows the differential travel times for the SPICeD and Asian data, and mean residuals are tabulated in Table 1. The mean for the SPICeD data is -0.12 s, and for the Asian data is -0.31 s. *Creager* [1999] reports similar, small ($<$0.4 s in magnitude) residuals for these paths with poorer coverage. The residuals are in the correct relative sense if PKP$_{DF}$ arrives early due to inner core anisotropy, and they show a weak dependence on ray angle with respect to the spin axis also suggestive of axisymmetric inner core anisotropy. To explore this effect further, we additionally correct the residuals for anisotropy using published models [*Creager*, 1992; *Song and Richards*, 1996; *Creager*, 1999]. Angles to the spin axis range from 45–60° for the SPICeD data and 61–79° for the Asian data (Fig. 2), which yield corrections larger than our measurement uncertainty for the SPICeD data. All models except one serve to reduce the travel time discrepancy between the two sets of observations. The best reduction, 66%, results from Creager's [1999] eastern hemisphere model. We thus find supportive evidence for inner core anisotropy, even though it is at the detection limit of the data.

The attenuation measurements, shown in Figure 3 against bottoming depth, do not reveal any trend with depth, nor do they show any significant difference in their mean values. A smoothed estimate of the trend suggests a depth variation, but it lies within the data scatter. The means are equal within their respective uncertainties: q is 103±53 for the SPICeD data and is 67±47 for the Asian data. The mean of all the data, and the best estimate for q is 77±51. This leads to a value for Q of 130^{+255}_{-52} for the bottoming range of the data, 140–340 km into the inner core. Our results compare favorably with *Niazi and Johnson* [1992], who found a $Q \approx 175$ for a similar depth range, and, within the broad uncertainty bounds, *Bhattacharyya*

et al. [1993] and *Tseng et al.* [2001]. It differs significantly from *Souriau and Roudil* [1995] and *Doornbos* [1974], both of whom found $Q \geq 450$ deeper than 225 km into the inner core.

Souriau and Romanowicz [1996, 1997] found an inverse relation between anisotropy and attenuation, with more attenuation associated with fast raypaths through the inner core. The trend was best displayed in regions where raypaths parallel the symmetry axis (in most models the Earth's spin axis). The patch of the inner core sampled in this study is at high latitude, so the nearest approach to axi-parallelism is 45°. On this account, the anisotropy signal is small, about +0.4 s [*Creager*, 1999]. Our own data, shown in Figure 4, do not require a q increase with δt.

Discussion

The insights of *Souriau and Romanowicz* [1996, 1997] prompted this study of the connection between anisotropy and attenuation to obtain constraints on the inner core's physical state. Though we can detect the influence of anisotropy on the differential travel times, we can not detect any correlation with attenuation within the limited resolution of the anisotropy signal in the dataset. Thus our results are similar to the global study of *Souriau and Romanowicz* [1997], where they also found no relation between anisotropy and attenuation at high latitudes.

The crossing-path design of our study, however, and the observational density (46 paths sampling the same region) provides a means to assess the relative contribution of meridional and axisymmetric anisotropy. Because the angle with respect to the spin axis is large, and the axisymmetric anisotropy contribution small, our observations also provide a strong test

of the idea that flow in the inner core, caused by the toroidal field, orients the inner core's crystallites [*Karato*, 1999; *Buffett and Bloxham*, 2000]. In particular, Maxwell stresses on the inner core should be greatest at middle latitudes in the inner core, where our ray paths cross. The bottoming azimuths of the Asian data lie in an extremely narrow range of $296\pm7°$, while the SPICeD data azimuths are $10\pm4°$, roughly orthogonal. The difference represents nearly the maximum expected amount of anisotropy if the fast axis parallels meridians of longitude. The difference in mean raw travel times is 0.19 seconds, and the average travel time across the inner core is 128 s in these data, which limits the anisotropy to 0.1%, or 0.6% within the widest limits represented by the uncertainty in the means. The small anisotropy we observe suggests that either the antisymmetric component of the toroidal field is small (in contrast to recent geodynamo simulations that yield strong fields in the core's interior [*Glatzmaier and Roberts*, 1995, 1996; *Kuang and Bloxham*, 1997, 1999]) or that the core's iron alloy does not have a sufficiently anisotropic magnetic susceptibility to orient it or to induce flow via the field [*Karato*, 1993, 1999]. The study region straddles the hemispheric boundary in the inner core separating the fast, eastern hemisphere from the slow, western hemisphere, so there is some contribution in the east-west paths from this factor. Thus the estimates should be viewed as upper bounds on meridional anisotropy.

Creager's [1999] dataset and the *Souriau and Romanowicz* [1997] non-equatorial data provide a complementary estimate of the amount of meridional anisotropy through the spread in the data at ray angles $\geq 50°$. The spread, estimated by eye, is about ±1 s, and is larger than what we observe in our study region. If this represents the maximum effect of meridional anisotropy, it corresponds to about 1.5% anisotropy. Our denser raypath sampling yields

lower, possibly much lower values, and in combination with the global data, suggests that meridional anisotropy is small in comparison with cylindrical, spin-axis-parallel anisotropy.

Conclusions

From a crossing-path study of PKP_{BC} and PKP_{DF} differential travel times in a restricted area of the inner core lying under Alaska, we find a difference in 0.19 s in east-west vs north-south path residuals, near the resolution limit of the data. Applying corrections for global inner core anisotropy decreases the path differences by up to 50%, consistent with it being an anisotropy signal. We also measured attenuation in the inner core along these different directions but found no differences in the east-west and north-south directions, and an average value for Q of of 130^{+255}_{-52} between 140–340 km depth. The data show no correlation between attenuation and travel time residuals. The small differences between travel time residuals along north-south and east-west paths bound meridional anisotropy to small values, between 0.1 and 0.6%. The small meridional component to anisotropy argues against significant contributions to anisotropy from low-order inner core convection or stresses imposed on the inner core by the outer core field.

Acknowledgements

References

M. I. Bergman, Measurements of electric anisotropy due to solidification texturing and the implications or theearth's inner core, *Nature*, *389*, 60–63, 1997.

J. Bhattacharyya, P. Shearer, and G. Masters, Inner-core attenuation from short-period PKP(BC) versus PKP(DF) wave-forms, *Geophys. J. Int.*, *114*, 1–11, 1993.

D. Bowers, D. McCormack, and D. Sharrock, Observations of PKP(DF) and PKP(BC) across the United Kingdom: implications for studies of attenuation in the Earth's core, *Geophys. J. Int.*, *140*, 2000.

B. A. Buffett and J. Bloxham, Deformation of earth's inner core by electromagnetic forces, *GRL*, *27*, 4001–4004, 2000.

V. F. Cormier, L. Xu, and G. L. Choy, Seismic attenuation of the inner core: Viscoelastic or stratigraphic?, *Geophys. Res lett.*, *25*, 4019–4022, 1998.

K. C. Creager, Anisotropy of the inner core from differential travel times of the phases PKP and PKIKP, *Nature*, *356*, 309–314, 1992.

K. C. Creager, Inner core rotation rate from small-scale heterogeneity and time-varying travel times, *Science*, *278*, 1284–1288, 1997.

K. C. Creager, Large-scale variations in inner core anisotropy, *J. Geophys. Res.*, *104*, 23127–23139, 1999.

D. Doornbos, The anelasticity of the inner core, *Geophys. J. Roy. astron. Soc.*, *38*, 397–415, 1974.

A. M. Dziewonski and F. Gilbert, The effect of small, aspherical perturbations on travel times and re-examination of the corrections for ellipticity, *Geophys. J. Roy. astron. Soc.*, *44*, 7–17, 1976.

B. Efron and R. Tibishrani, Statistical data analysis in the computer age, *Science*, *253*, 390–395, 1991.

D. R. Fearn, D. E. Loper, and P. H. Roberts, Structure of the earth's inner core, *Nature*, *292*, 232–233, 1981.

G. A. Glatzmaier and P. H. Roberts, A three-dimensional convective dynamo solution with rotating and finitely conducting inner core and mantle, *Phys. Earth and Planet. Int.*, *91*, 63–75, 1995.

G. A. Glatzmaier and P. H. Roberts, An anelastic evolutionary geodynamo simulation driven by compositional and thermal convection, *Physica D*, *97*, 81–94, 1996.

R. Jeanloz and H. R. Wenk, Convection and anisotropy of the inner core, *Geophys. Res. Lett.*, *15*, 72–75, 1988.

S. Kaneshima, Mapping heterogeneity of the uppermost inner core using two pairs of core phases, *Geophys. Res. Lett.*, *23*, 3075–3078, 1996.

S.-I. Karato, Inner-core anisotropy due to the magnetic-field-induced preferred orientation of iron, *Science*, *262*, 1708–7111, 1993.

S.-I. Karato, Seismic anisotropy of the earth's inner core resulting from flow induced by maxwell stresses, *Nature*, *402*, 871–873, 1999.

J.-M. Kendall and G. Helffrich, SPICeD: imaging the deep Earth, *Astron. and Geophys.*, *42*, 3.26–3.29, 2001.

J.-M. Kendall and P. G. Silver, Constraints from seismic anisotropy on the nature of the lowermost mantle, *Nature*, *381*, 409–412, 1996.

B. L. N. Kennett, E. R. Engdahl, and R. Buland, Constraints on seismic velocities in the Earth from traveltimes, *Geophys. J. Int.*, *122*, 108–124, 1995.

W. Kuang and J. Bloxham, An Earth-like numerical dynamo model, *Nature*, *389*, 371–374, 1997.

W. Kuang and J. Bloxham, Numerical modelling of magnetohydrodynamic convection in a rapidly-rotating spherical shell: Weak and strong field dynamo action, *J. Comp. Phys.*, *153*, 51–81, 1999.

D. E. Loper and D. R. Fearn, A seismic model of a partially molten inner core, *J. Geophys. Res*, *88*, 1235–1242, 1983.

M. Niazi and L. R. Johnson, *Q* in the inner core, *Phys. Earth and Planet. Int.*, *74*, 55–62, 1992.

F. L. Niu and L. X. Wen, Hemispherical variations in seismic velocity at the top of the earth's inner core, *Nature*, *410*, 1081–1084, 2001.

J. Park, C. R. Lindberg, and F. L. Vernon III, Multitaper spectral analysis of high-frequency seismograms, *J. Geophys. Res*, *92*, 12675–12684, 1987.

S. Peacock and J. A. Hudson, Seismic properties of rocks with distributions of small cracks, *Geophys. J. Int.*, *102*, 471–484, 1990.

W. H. Press, B. P. Flannery, S. A. Teukolsky, and W. T. Vetterling, *Numerical Recipes in Fortran*, Cambridge University Press, Cambridge, 1992.

B. Romanowicz, X.-D. Li, and J. Durek, Anisotropy of the inner core: Could it be due to low order convection?, *Science*, *274*, 963–966, 1996.

I. S. Sacks, Anelasticity of the inner core, *Annual Report of the Director, Dept. of Terrestrial Magnetism*, *1969-1970*, 416pp, 1971.

X. Song, Joint inversion for inner core rotation, inner core anisotropy, and mantle heterogeneity, *J. Geophys. Res.*, *105*, 7931–7943, 2000.

X. Song and P. G. Richards, Seismological evidence for differential rotation of the Earth's inner core, *Nature*, *382*, 221–224, 1996.

A. Souriau and B. Romanowicz, Anisotropy in inner core attenuation: A new type of data to constrain the nature of the solid core, *Geophys. Res. Lett.*, *23*, 1–4, 1996.

A. Souriau and B. Romanowicz, Anisotropy in the inner core: Relation between P-velocity and attenuation, *Phys. Earth and Planet. Int.*, *101*, 33–47, 1997.

A. Souriau and P. Roudil, Attenuation in the uppermost inner core from broad-band GEOSCOPE *PKP* data, *Geophys. J. Int.*, *123*, 572–587, 1995.

W.-J. Su and A. M. Dziewonski, Inner core anisotropy in three dimensions, *J. Geophys. Res.*, *100*, 9831–9852, 1995.

S. Tanaka and H. Hamaguchi, Degree one heterogeneity and hemispherical variation of anisotropy in the inner core from PKP_{BC}-PKP_{DF} times, *J. Geophys. Res.*, *102*, 2925–2938, 1997.

T.-L. Tseng, B.-S. Huang, and B.-H. Chin, Depth-dependent attenuation in the uppermost inner core from the Taiwan short-period seismic array PKP data, *Geophys. Res. Lett.*, *28*, 459–462, 2001.

M. Weber and P. Machetel, Convection within the inner-core and thermal implications, *Geophys. Res. Lett.*, *19*, 2107–2110, 1992.

R. Widmer, G. Masters, and F. Gilbert, Spherically symmetrical attenuation within the earth from normal mode data, *Geophys. J. Int.*, *104*, 541–553, 1991.

G. Helffrich and S. Kaneshima, Earth and Planetary Sciences, Tokyo Institute of Technology, 2-12-1 Ookayama, Meguro-ku, Tokyo 152-8551, Japan

J.-M. Kendall, Earth Sciences, University of Leeds, Leeds, UK

Received _____

[1]also at Earth Sciences, University of Bristol, Bristol, UK

Table 1. Averaged PKP$_{BC}$-PKP$_{DF}$ travel times, reduced to AK135

			Anisotropy corrections			
	#obs	Raw[e]	Cre92[a]	S&R96[b]	Cre99[c]	Cre99[d]
SPICeD	13	-0.124	-0.592	-0.298	0.033	-0.527
		±0.220	±0.281	±0.226	±0.251	±0.215
Asian	33	-0.311	-0.396	-0.465	0.125	-0.590
		±0.373	±0.372	±0.377	±0.352	±0.387
diff.		0.187	-0.196	0.167	-0.092	0.063

[a]–*Creager* [1992]; [b]–*Song and Richards* [1996], time invariant;

[c]–*Creager* [1999], western hem.; [d]–*Creager* [1999], eastern hem. [e]–Times

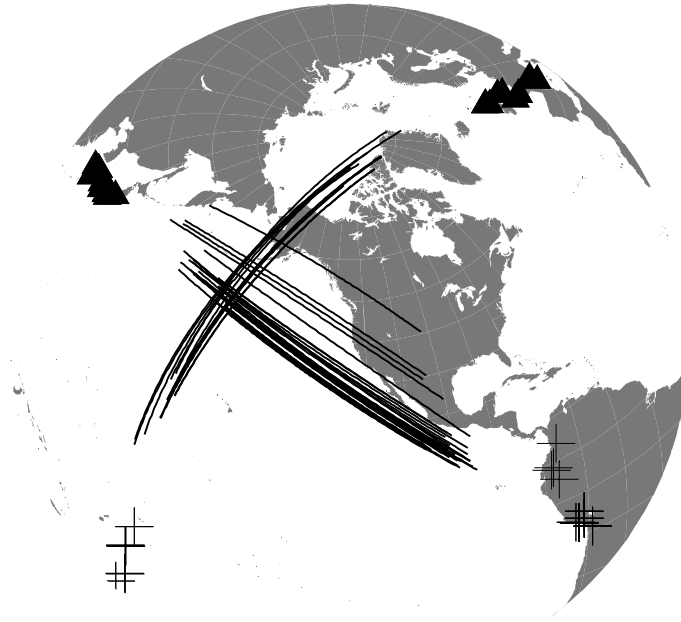corrected for ellipticity [*Dziewonski and Gilbert*, 1976].

Figure 1. Map of ray paths of PKP$_{DF}$ through the inner core. Triangles indicate stations, crosses indicate sources. Northerly paths are Tonga-Fiji to the UK and western Europe, and east-west paths are S. America to east Asia. S. American source regions are between -18.917 and 3.823° lat. and -77.995 and -69.141° lon., and Tonga-Fiji events between -31.511 and -15.948° lat. and 179.725 182.562° lon. and occurred in 1995-2001.
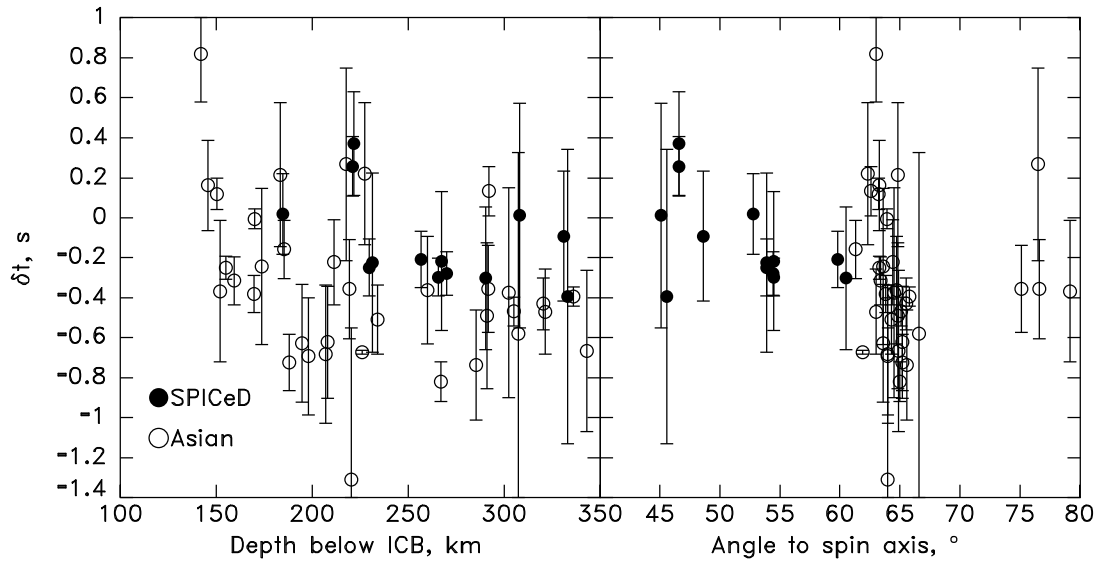
Figure 2. Raw PKP$_{BC}$-PKP$_{DF}$ residuals with respect to the AK135 model, corrected for ellipticity, against bottoming depth in the inner core (*left*) and angle with respect to the rotation axis (*right*). SPICeD data indicate Tonga-Fiji to the UK and western Europe, and Asian data east-west paths from S. America to eastern Asia. Trend to positive residuals with decreasing angle suggests axi-symmetric inner core anisotropy is responsible for the difference in means for the two paths.
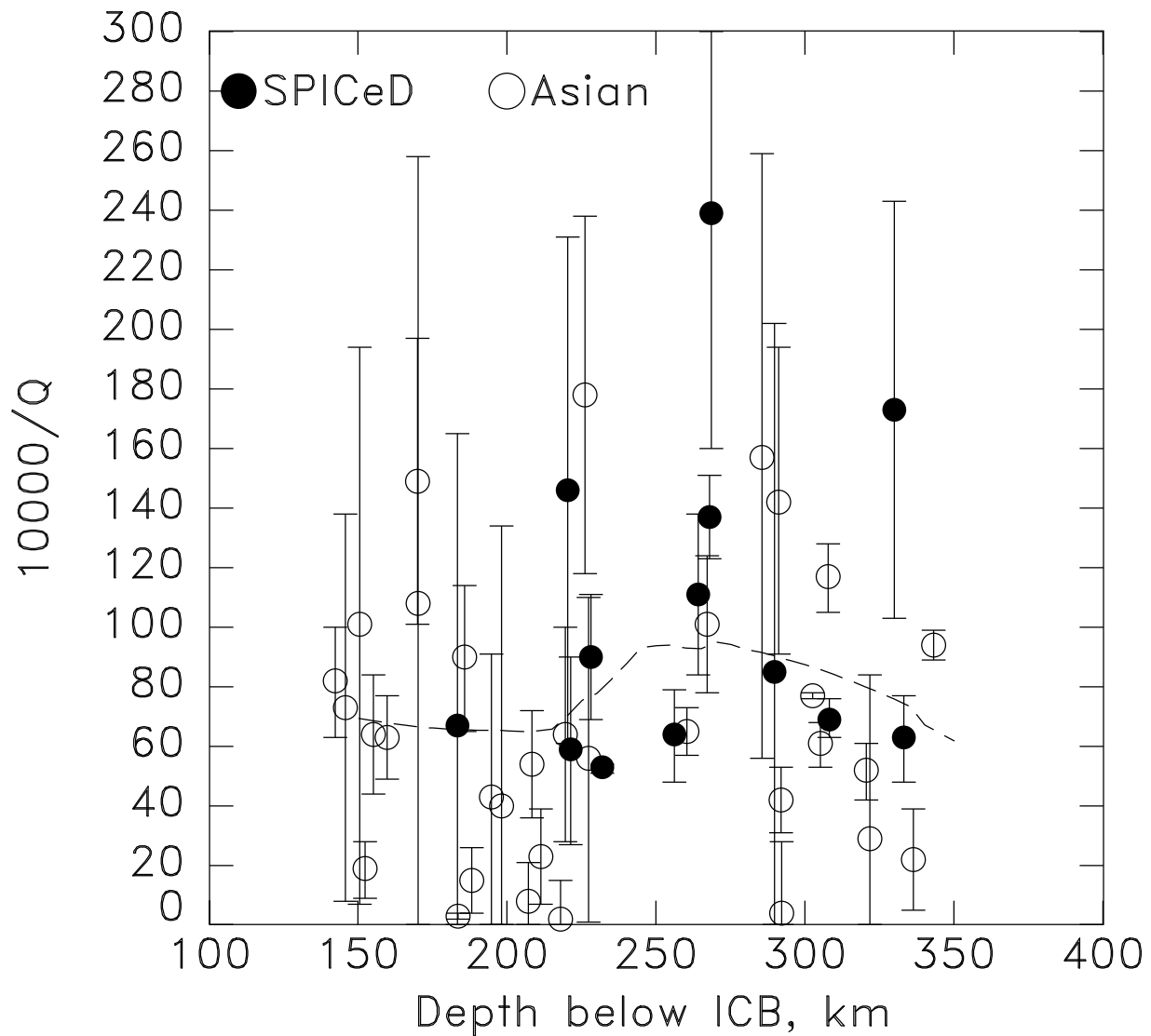
Figure 3. Estimated $q \equiv 10000/Q$ values for the two datasets against bottoming depth in the inner core. SPICeD data indicate Tonga-Fiji to the UK and western Europe, and Asian data east-west paths from S. America to eastern Asia. Mean values are $q = 105 \pm 53$ and $q = 67 \pm 47$ for SPICeD and Asian data, respectively. Dashed line is a smoothed estimate of the depth variation, but it does not vary outside the bounds of the average of the whole data, $q = 77 \pm 51$.
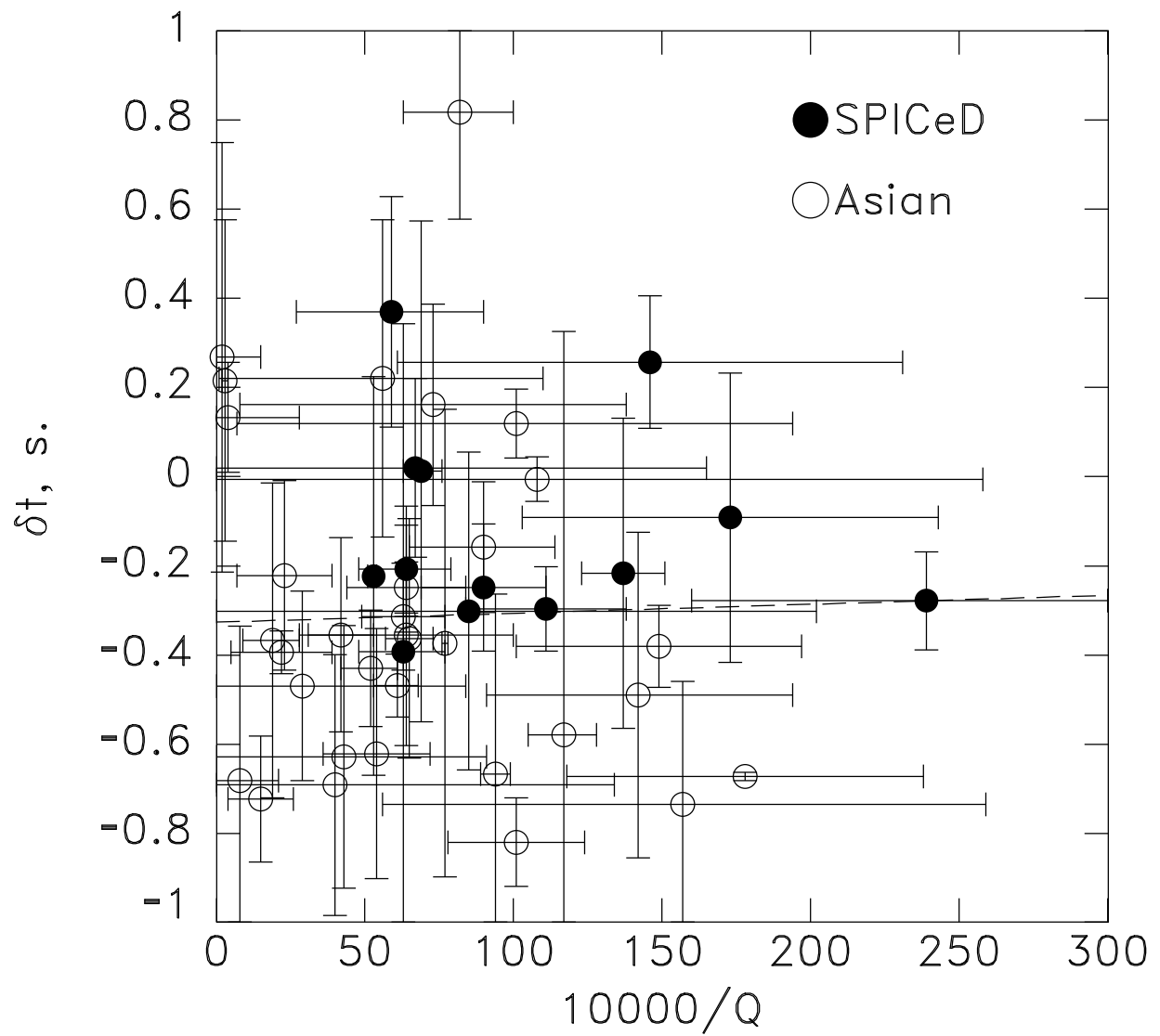
Figure 4. Scatterplot of q values versus δt for individual seismograms in the two datasets.

Dashed line is robust linear fit of the trend of the data, suggesting no correlation between the

widely-scattered values.